CHAPTER 4

Properties of Carbon Fibers

Introduction

The properties of carbon fibers vary widely depending on the structure (Chapter 3) of the fibers. In general, attractive properties of carbon fibers include the following:

- low density
- high tensile modulus and strength
- low thermal expansion coefficient
- thermal stability in the absence of oxygen to over 3 000°C
- excellent creep resistance
- chemical stability, particularly in strong acids
- biocompatibility
- high thermal conductivity
- low electrical resistivity
- availability in a continuous form
- decreasing cost (versus time)

Disadvantages of carbon fibers include the following:

- anisotropy (in the axial versus transverse directions)
- low strain to failure
- compressive strength is low compared to tensile strength
- tendency to be oxidized and become a gas (e.g., CO) upon heating in air above about 400°C
- oxidation of carbon fibers is catalyzed by an alkaline environment

As each property is determined by the structure, the different properties are interrelated. The following trends usually go together:

- increase in the tensile modulus
- decrease in the strain to failure
- decrease in the compressive strength

- increase in the shear modulus
- increase in the degree of anisotropy
- decrease in the electrical resistivity
- increase in the thermal conductivity
- decrease in the coefficient of thermal expansion
- increase in density
- increase in thermal stability (oxidation resistance)
- increase in chemical stability
- increase in cost

Mechanical Properties

Table 4.1 [1] shows the tensile properties of carbon fibers along the fiber axis compared to those of a graphite single crystal along the *a*-axis, i.e., parallel to the carbon layers. Although the carbon layers in a carbon fiber exhibit a strong preferred orientation parallel to the fiber axis, the alignment of the layers is far from being perfect and the crystallite size is finite. Therefore, the tensile modulus and strength of carbon fibers are considerably below those of a graphite single crystal. The modulus of HM-type fibers approaches that of a graphite single crystal, but that of HT-type fibers is much below that of a graphite single crystal. The tensile strengths of both HM and HT fibers are very much below that of a graphite single crystal, although the strength of HT is higher than that of HM. There is thus much room for improvement of the tensile strength of carbon fibers. In contrast, there is not much room to improve the tensile modulus.

The tensile properties of some commercial carbon fibers of the high-performance (HP) grade are shown in Table 4.2 [2]. For the same precursor material (PAN or mesophase pitch), the tensile strength, modulus, and strain to failure vary over large ranges.

The tensile modulus is governed by the preferred orientation of the carbon layers along the fiber axis, so it increases with decreasing interlayer

Table 4.1 Considerations concerning Young's modulus (E) and the tensile strength (σ) of carbon fibers. From Ref. 1.

	Theoretical values for graphite single crystal	*Carbon fibers*		
		HT type	*HM type*	*Future trends*
Young's modulus, E	E = 1 000 GPa	E = 250 GPa	E = 700 GPa	Further increase not necessary
Tensile strength, σ	$\sigma_{theor.} = E/10$ = 100 GPa	$\sigma_{theor.}$ = 25 GPa $\sigma_{exp.}$ = 5 GPa = 20% of $\sigma_{ther.}$	$\sigma_{theor.}$ = 70 GPa $\sigma_{exp.}$ = 3 GPa = 4% of $\sigma_{theor.}$	Further improvement expected

Table 4.2 Tensile modulus, strength, and strain to failure of carbon fibers. From Ref. 2.

Manufacturer	*Fiber*	*Modulus (GPa)*	*Strength (GPa)*	*Strain to failure (%)*
PAN-based, high modulus (low strain to failure)				
Celanese	Celion GY-70	517	1.86	0.4
Hercules	HM-S Magnamite	345	2.21	0.6
Hysol Grafil	Grafil HM	370	2.75	0.7
Toray	M50	500	2.50	0.5
PAN-based, intermediate modulus (intermediate strain to failure)				
Celanese	Celion 1000	234	3.24	1.4
Hercules	IM-6	276	4.40	1.4
Hysol Grafil	Apollo IM 43-600	300	4.00	1.3
Toho Beslon	Sta-grade Besfight	240	3.73	1.6
Amoco	Thornel 300	230	3.10	1.3
PAN-based, high strain to failure				
Celanese	Celion ST	235	4.34	1.8
Hercules	AS-6	241	4.14	1.7
Hysol Grafil	Apollo HS 38-750	260	5.00	1.9
Toray	T 800	300	5.70	1.9
Mesophase pitch-based				
Amoco	Thornel P-25	140	1.40	1.0
	P-55	380	2.10	0.5
	P-75	500	2.00	0.4
	P-100	690	2.20	0.3
	P-120	820	2.20	0.2

spacing (d_{002}) and with increasing L_c and L_a, as shown in Table 4.3 [3] for a series of mesophase pitch-based carbon fibers produced by du Pont.

Comparison of the du Pont fibers (Table 4.3) with the Amoco fibers (Table 4.2), both of which are based on mesophase pitch, indicates the superior tensile strength of the du Pont fibers. Unfortunately the du Pont fibers are not commercially available, whereas the Amoco fibers are.

Figure 4.1 [4] shows the tensile stress–strain curves of carbon fibers with different values of the tensile modulus. For a high-modulus carbon fiber (e.g., HM70), the stress–strain curve is a straight line up to failure; as the modulus decreases there is an increasing tendency for the slope to increase with increasing strain. This effect occurs because the fiber is increasingly stretched as the strain increases; the carbon layers become more aligned and the modulus therefore increases. It forms the basis of a process called stress-graphitization.

Table 4.3 Mechanical properties of pitch-based carbon fibers and their structural parameters as determined by X-ray diffraction: d_{002}, the interlayer spacing; L_c, the out-of-plane crystallite size; and L_a, the in-plane crystallite size parallel to the fiber axis. From Ref. 3.

Fibers	*Tensile modulus (GPa)*	*Tensile strength (GPa)*	d_{002} *(nm)*	L_c *(nm)*	L_a *(nm)*
E-35	241	2.8	0.3464	3.2	7.2
E-55	378	3.2	0.3430	8.2	16.2
E-75	516	3.1	0.3421	10.7	22.4
E-105	724	3.3	0.3411	17.3	46.1
E-120	827	3.4	0.3409	18.9	51.4
E-130	894	3.9	0.3380	24.0	180.4

The tensile strength is strongly influenced by flaws, so it increases with decreasing test (gage) length and with decreasing fiber diameter. Figure 4.2 shows the variation of the tensile strength with the fiber diameter for various PAN-based carbon fibers [5]. There are two types of flaws, namely surface flaws and internal flaws. The surface flaws control the strength of carbon fibers that have not been heat-treated above 1 000–1 200°C; the internal flaws control the strength of carbon fibers that have been heat-treated above 1 000–1 200°C [6]. Upon etching a fiber, the amount of surface flaws is decreased, causing the fiber strength to increase. The minimum practical gage length is 0.5 mm [7], even though the ultimate fragment length of a stressed single fiber composite is 0.3 mm [6] and it is the ultimate fragment length (also called the critical length) that determines the composite strength. Table 4.4 [7] shows the tensile

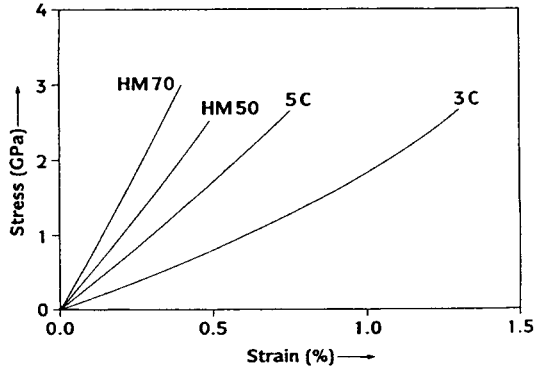

Figure 4.1 Tensile stress–strain curves of pitch-based carbon fibers (Carbonic HM50 and HM70) and PAN-based carbon fibers (Fortafil 3C and 5C). The test (gage) length is 100 mm. The strain rate is 1%/min. From Ref. 4. (Reprinted with permission from Pergamon Press Ltd.)

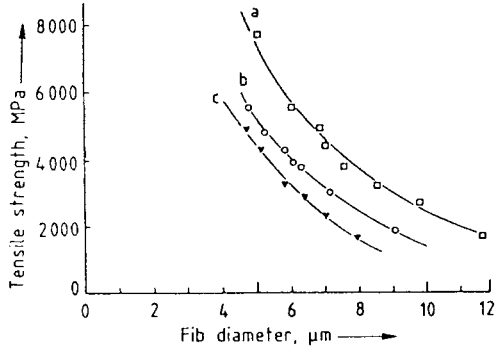

Figure 4.2 Relation between the tensile strength and fiber diameter: (a) Hercules AS-4 (Type HT), (b) Torayca T-300 (Type HT), and (c) Torayca M40 (Type HM). From Ref. 5.

strengths of carbon fibers (Hercules AS-4, PAN based) at different gage lengths, as determined by traditional tensile testing and by in situ fiber strength testing. The latter testing method involves embedding a single fiber in a matrix (e.g., epoxy) and pulling the unembedded ends of the fiber to increasing strain levels up to approximately three times greater than the failure strain of the fiber. While the strain is gradually increased, the number of breaks in the fiber is counted in situ [7]. The fiber eventually breaks into fragments of a length equal to the critical length, which is related to the tensile properties of the fiber and the interfacial shear strength between the fiber and the matrix. Table 4.4 shows that the fiber strength determined by either method increases with decreasing gage length. The latter method has the advantage of being

Table 4.4 Tensile strengths of AS-4 fibers at different gage lengths as determined by traditional tension testing and by in situ fiber strength testing in epoxy and solvent-deposited polycarbonate matrices. Tensile strengths appear in MPa followed by standard deviations. From Ref. 7.

Gage length (mm)	*Conventional tension test (MPa)*	*In situ strength (MPa)*	
		Epoxy	*Polycarbonate*
25.4	3 215 ± 966	3 188 ± 704	2 698 ± 518
8.0		3 850 ± 738	3 347 ± 725
4.0		4 264 ± 787	3 733 ± 752
2.0		4 720 ± 856	4 175 ± 773
1.0	5 285 ± 1 731	5 223 ± 911	4 582 ± 814
0.55	5 644 ± 994	5 693 ± 945	4 996 ± 869
0.3		6 189 ± 973	5 437 ± 883

Table 4.5 Tensile and compressive strength of carbon fibers. From Ref. 8.

	Pitch-based		*PAN-based*	
Carbon fiber	*Carbonized fiber HTX*	*Graphitized fiber HMX*	*Carbonized fiber T-300*	*Graphitized fiber M40*
Tensile strength $(\sigma_f)_{ten.}$ (GPa)	3.34	4.33	3.50	2.88
Estimated compressive strength $(\sigma_f)_{comp.}$ (GPa)	1.25	0.54	2.06	0.78
$(\sigma_f)_{comp.}/(\sigma_f)_{ten.}$ (%)	37.4	12.5	58.9	27.1

Table 4.6 Compressive failure strains for pitch-based fibers and PAN-based carbon fibers. From Ref. 9.

Precursor	*Fiber*	*Modulus (GPa)*	*Mean failure strain (%)*	*Standard deviation (%)*	*No. of specimens*
Pitch	HM	519	0.346	0.074	39
	HT	244	0.981	0.064	9
	UHM	662	0.163	0.063	9
	P-75	517	0.248	0.04	8
PAN	AS-1	228	2.59	0.181	8
	AS-4	241	2.27	0.256	8
	IM-6	276	2.35	0.132	8
	IM-7	303	2.11	0.317	8
	T-700	234	2.66	0.111	8
	T-300	230	2.36	0.125	8
	GY-30	241	2.65	0.207	8

applicable to very short gage lengths, but it has the disadvantage of being sensitive to the fiber prestrain resulting from the specimen preparation technique. The difference between the in situ fiber strengths for epoxy and polycarbonate matrices (Table 4.4) is due to a difference in the fiber prestrain.

The compressive strength is much lower than the tensile strength, as shown in Table 4.5 [8]. The ratio of the compressive strength to the tensile strength is smaller for graphitized fibers than carbonized fibers. Pitch-based carbon fibers have even lower compressive strength than PAN-based fibers. Moreover, the compressive failure strain is much lower for pitch-based carbon fibers than PAN-based carbon fibers, as shown in Table 4.6 [9]. These differences between pitch-based and PAN-based fibers are consistent with the

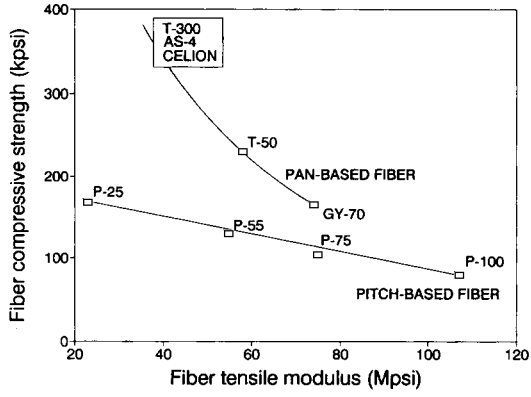

Figure 4.3 Relation between the compressive strength and tensile modulus of carbon fibers. From Ref. 11. (By permission of the Materials Research Society.)

difference in the compressive failure mechanism. Pitch-based fibers of high modulus typically deform by a shear mechanism, with kink bands formed on a fracture surface at 45° to the fiber axis. In contrast, PAN-based fibers typically buckle on compression and form kink bands at the innermost part of the fracture surface, which is normal to the fiber axis [10]. The difference in compressive behavior between pitch-based and PAN-based carbon fibers is attributed to the strong preferred orientation of the carbon layers in pitch-based fibers and the more random microstructure in PAN-based fibers. The oriented layer microstructure causes the fiber to be susceptible to shearing [9]. Thus, the compressive strength decreases with increasing tensile modulus, as shown in Figure 4.3 [11]. The axial Poisson's ratio of carbon fibers is around 0.26–0.28 [12].

The shear modulus of carbon fibers decreases with increasing L_c and with increasing L_a [4]. This is expected, since increases in L_c and L_a imply a greater degree of carbon layer preferred orientation. A decrease in the shear modulus is accompanied by a decrease in the compressive strength, as shown in Figure 4.4 [4]. The values of the shear modulus of various commercial carbon fibers are listed in Table 4.7 [13].

The values of the torsional modulus of various commercial carbon fibers are listed in Table 4.8 [6]. The torsional modulus is governed mostly by the cross-sectional microstructure. Mesophase pitch-based carbon fibers have low torsional modulus because they have an appreciable radial cross-sectional microstructure, which facilitates interlayer shear. Hence, the torsional modulus of mesophase pitch-based carbon fibers is even lower than that of isotropic pitch-based carbon fibers. On the other hand, PAN-based carbon fibers have high torsional modulus because they have an appreciable degree of circumferential microstructure [6].

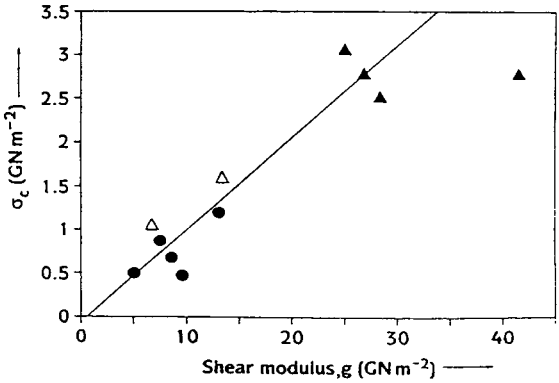

Figure 4.4 Relation between the compressive strength (σ_c) and the shear modulus (g) of carbon fibers. From Ref. 4. (Reprinted with permission from Pergamon Press Ltd.)

Table 4.7 Properties of some PAN-based carbon fibers. From Ref. 13.

Fiber	*Tensile modulus (GPa)*	*Tensile strength (GPa)*	*Shear modulus (GPa)*
T-300	230	3.5	17.0
M30	290	3.9	17.0
T-50	390	2.4	
M-40	400	2.7	15.8
M-46	450	2.35	14.8
GY-70	520	1.8	
T-800H	290	5.6	18.1
M-40J	390	4.3	17.0
M-46J	450	4.2	17.0
M-60J	585	3.8	

Electrical Properties

The electrical resistivity of the mesophase pitch-based carbon fibers of Table 4.3 is shown as a function of temperature from 2 to 300 K in Figure 4.5 [3]. The resistivity decreases with increasing temperature for each type of fiber. This is because the carrier density increases with temperature, just as for carbons and graphites in general. At a given test temperature, the resistivity decreases with increasing tensile modulus. This is because an increase in the tensile modulus is accompanied by a decrease in the concentration of defects, and defects cause carrier scattering.

Table 4.8 Torsional modulus and Young's modulus of various carbon fiber types. From Ref. 6.

Carbon fiber type	*Young's modulus (GPa)*	*Torsional modulus (GPa)*
Pitch mesophase		
PM-A	184	13.5
PM-B	262	9.0
		9.2
PM-C	364	10.8
		9.7
PM-C (1700)	400	10.4
Isotropic pitch		
KCF-200	80	16.4
KCF-2700	~80	18.0
PAN		
T-400	226	21.4
AS	215	21.0
HM-S(H)	~370	20.2
Modmor I	~400	28.2
HM-S(C)	~380	35.3
Rayon		
T-11 (carbon)	79	15.3
T-12 (graphite)	83	22.8
T-25	176	12.3
T-70	390	12.3
T-75	540	13.8
T-100	680	16.9

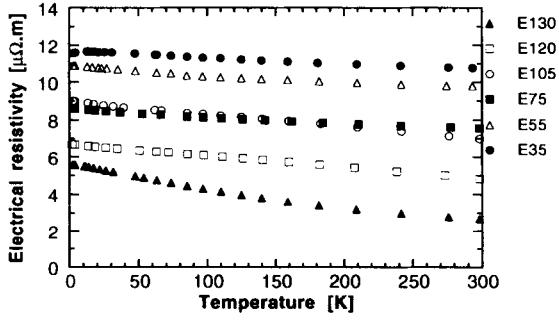

Figure 4.5 Variation of the electrical resistivity with temperature for the carbon fibers of Table 4.2. From Ref. 3. (By permission of IOP Publishing Limited.)

Table 4.9 Effect of nickel coating on the properties of PAN-based AS-4 (Hercules) carbon fiber. From Ref. 16.

Property	*Bare fiber*	*Ni-coated fiber*
Diameter (μm)	7.0	7.8
Density (g/cm^3)	1.80	2.97
Electrical resistivity ($10^{-6}\Omega$.cm)	1 530	7
Thermal conductivity (W/m/K)	7.2	10.7
Thermal expansion coefficient (10^{-6}/°C)	−1.7	−0.8
Tensile modulus (GPa)	234	210
Tensile strength (MPa)	3 582	2 582
Tensile elongation (%)	1.53	1.33

An effective way to decrease the resistivity of carbon fibers by a factor of up to 10 is intercalation. Intercalation is the formation of layered compounds in which foreign atoms (called the intercalate) are inserted between the carbon layers. The intercalate acts as an electron acceptor or an electron donor, thus doping the carbon fibers. This doping causes the carrier concentration to increase, thereby decreasing the electrical resistivity. Intercalation is only possible in relatively graphitic carbon fibers. For example, bromination (i.e., intercalation with bromine, an acceptor) causes a weight uptake of 18–20% for Amoco's Thornel P-100 and P-75 fibers, but 0% for P-55; it causes a resistivity decrease of 73–79% for P-120, P-100, and P-75 fibers, but just 4% for P-55 [14]. For the case of brominated P-100-4 (P-100-4 is even more graphitic than P-100), a resistivity of 11.0 $\mu\Omega$.cm has been reported [6]. On the other hand, the severity of the intercalation reaction in highly graphitic fibers can cause physical damage to the fibers, so that the mechanical properties and oxidation resistance are degraded [15]. Therefore, there is an optimum degree of graphitization, which corresponds to that of P-100 fibers for the case of bromine as the intercalate [14]. The low electrical resistivity of intercalated carbon fibers makes these fibers useful in composites for electromagnetic interference shielding.

A way to decrease the electrical resistivity and increase the thermal conductivity of carbon fibers is to coat the fibers with a metal that is more conductive than the fibers. All types of carbon fibers are higher in electrical resistivity than metals, therefore all metal-coated carbon fibers are more electrically conductive than the corresponding bare carbon fibers. However, the thermal conductivities of the highly graphitic carbon fibers, such as pitch-based Thornel P-100, P-120, and K1100X fibers of Amoco, are even higher than copper. Thus, metal-coated carbon fibers are superior to the corresponding bare fibers in thermal conductivity only for the less graphitic fibers, which constitute the vast majority of carbon fibers used in practice anyway. Table 4.9 [16] shows the effect of a 0.35 μm thick electrodeposited

Table 4.10 Thermal properties of the most advanced pitch-based carbon fibers. From Ref. 17.

Material	*Longitudinal thermal conductivity (W/m/K)*	*CTE (10^{-6}/K)*	*Density (g/cm^3)*	*Specific conductivity (W.cm^3/m/K/g)*
Al-6063	218	23	2.7	81
Copper	400	17	8.9	45
P-100	520	−1.6	2.2	236
P-120	640	−1.6	2.1	305
K1100X	1 100	−1.6	2.2	500
K1100X/Al (55 vol.%)	634	0.5	2.5	236
K1100X/epoxy (60 vol.%)	627	−1.4	1.8	344
K1100X/Cu (46 vol.%)	709	1.1	5.9	117
K1100X/C (53 vol.%)	696	−1.0	1.8	387

nickel coating on the properties of an originally 7.0 μm thick PAN-based AS-4 carbon fiber (Hercules), which is not graphitic. The nickel coating causes the density to increase, the electrical resistivity to decrease, the thermal conductivity to increase, the thermal expansion coefficient to increase, and the tensile modulus, strength, and elongation to decrease. The largest effect is the decrease in the electrical resistivity.

Thermal Conductivity

The longitudinal thermal conductivity, thermal expansion coefficient, density, and specific thermal conductivity (conductivity/density) of Amoco's mesophase pitch-based carbon fibers are shown in Table 4.10 [17]. The thermal conductivities of P-100, P-120, and K1100X fibers are all higher than that of copper, while the thermal expansion coefficients and densities are much lower than those of copper. Thus, the specific thermal conductivity is exceptionally high for these carbon fibers. In general, the thermal expansion coefficient of carbon fibers decreases with increasing tensile modulus, as shown in Figure 4.6 [18]. Table 4.10 also shows that use of K1100X fibers in Al, epoxy, Cu and C matrices results in composites of high thermal conductivity.

Oxidation Resistance

The oxidation resistance of carbon fibers increases with the degree of graphitization. Figure 4.7 shows the percentage weight remaining as a function of temperature during exposure of carbon fibers to flowing air for three types

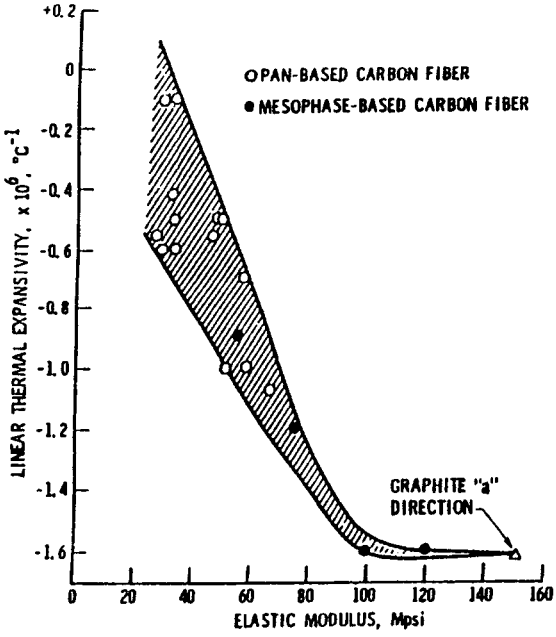

Figure 4.6 Relation between the longitudinal thermal expansion coefficient and the tensile modulus of carbon fibers. From Ref. 18.

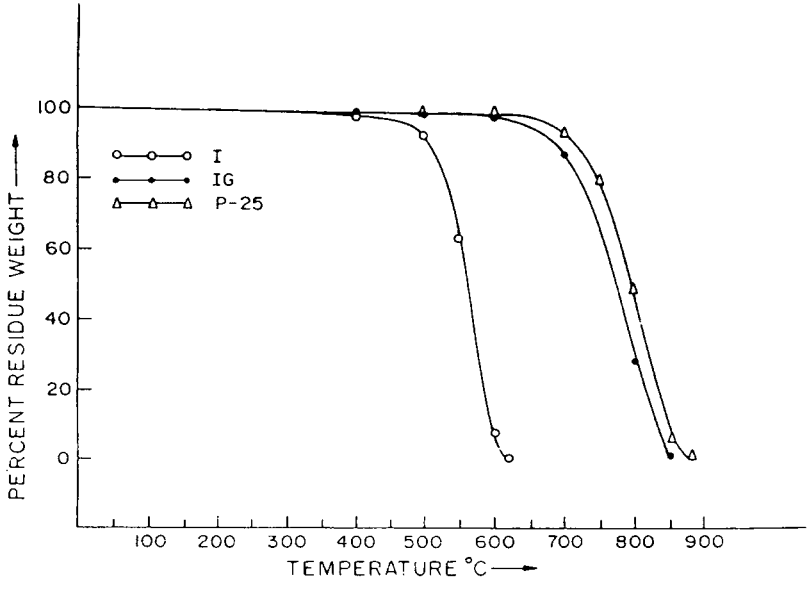

Figure 4.7 Percent residual weight during heating (in flow air) of three types of pitch-based carbon fibers. From Ref. 19. (Reprinted with permission from Pergamon Press Ltd.)

of fibers, namely I (Kureha isotropic pitch-based carbon fibers), IG (Kureha isotropic pitch-based carbon fibers graphitized at 2 700°C) and P-25 (Amoco mesophase pitch-based carbon fibers) [19]. In the case of I fibers, weight loss starts at about 400°C and is gradual up to 500°C; from 500 to 600°C, the weight loss is sharp; complete weight loss takes place at 620°C. In the case of IG fibers, weight loss starts at about 400°C, but is gradual up to 700°C; beyond 700°C, the weight loss is sharp; complete weight loss takes place by 850°C. In the case of P-25 fibers, weight loss starts at about 500°C and is only about 2% up to 600°C; complete weight loss takes place at about 880°C. The apparent activation energies range from 112 to 205 kJ/mol for various pitch-based carbon fibers [19]. The oxidation has been modeled to yield information on the oxidation kinetics, the activation energy, and the rate-determining step [20].

Severe oxidation causes carbon fibers to lose weight due to the evolution of CO or CO_2 gases. However, slight oxidation may cause carbon fibers to gain weight slightly due to the formation of chemical bonds to various oxygen-containing functional groups on the surface of the fibers. The oxygen-containing groups (or adsorbed oxygen) increase the polar component of the surface free energy and hence result in enhanced electrochemical response (relevant for fiber electrodes) and improved fiber–matrix bonding (when the fibers are used in a composite).

Although oxidation due to molecular oxygen is most common on earth, oxidation due to atomic oxygen is important in aerospace applications. Atomic oxygen is more reactive than molecular oxygen and is the dominant atmospheric element in low earth orbit [21].

Biocompatibility

Carbon is more biocompatible than even gold or platinum, so carbon fibers are used as implants, which act as a scaffold for collagen in tendons [22], for the repair of abdominal wall defects [23], and for the growth of spinal axons in a spinal cord [24]. The carbon fibers provide a favorable adhesive surface and a possible guiding function [24].

References

1. E. Fitzer and F. Kunkele, *High Temp. – High Pressures* **22**(3), 239–266 (1990).
2. D.J. Johnson, *J. Phys. D: Appl. Phys.* **20**(3), 286–291 (1987).
3. B. Nysten, J.-P. Issi, R. Barton, Jr., D.R. Boyington, and J.G. Lavin, *J. Phys. D: Appl. Phys.* **24**(5), 714–718 (1991).
4. M.G. Northolt, L.H. Veldhuizen, and H. Jansen, *Carbon* **29**(8), 1267–1279 (1991).
5. E. Fitzer and W. Frohs, *Chem. Eng. Technol.* **13**(1), 41–49 (1990).
6. J.-B. Donnet and R.C. Bansal, *International Fiber Science and Technology 10 (Carbon Fibers)*, 2d ed., Marcel Dekker, New York, 1990, pp. 267–366.
7. M.C. Waterbury and L.T. Drzal, *J. Compos. Technol. Res.* **13**(1), 22–28 (1991).

8. T. Ohsawa, M. Miwa, M. Kawade and E. Tsushima, *J. Appl. Polym. Sci.* **39**(8), 1733–1743 (1990).
9. J.M. Prandy and H.T. Hahn, in *Proc. Int. SAMPE Symp. and Exhib., 35, Advanced Materials: Challenge Next Decade*, edited by G. Janicki, V. Bailey, and H. Schjelderup, 1990, pp. 1657–1670.
10. D.J. Johnson, in *Carbon Fibers Filaments and Composites*, edited by J.L. Figueiredo, C.A. Bernardo, R.T.K. Baker, and K.J. Huttinger, Kluwer Academic, Dordrecht, 1990, pp. 119–146.
11. S. Kumar and T.E. Helminiak, *Mater. Res. Soc. Symp. Proc., Vol. 134 (Mater. Sci. Eng. Rigid-Rod Polym.*, 1989, 363–374.
12. I. Krucinska and T. Stypka, *Compos. Sci. Technol.* **41**, 1–12 (1991).
13. S. Kumar, in *Proc. Int. SAMPE Symp. and Exhib., 35, Advanced Materials: Challenge Next Decade*, edited by G. Janicki, V. Bailey, and H. Schjelderup, 1990, pp. 2224–2235.
14. D.D.L. Chung, *Ext. Abstr. Program Bienn. Conf. Carbon* **20**, 694–695 (1991).
15. C.T. Ho and D.D.L. Chung, *Carbon* **28**(6), 831–837 (1990).
16. R.E. Evans, D.E. Hall, and B.A. Luxon, *SAMPE Q.* **17**(4), 18–26 (1986).
17. Amoco Performance Products, data sheet, April 30, 1992.
18. W. de la Torre, in *Proc. 6th Int. SAMPE Electron. Conf.*, 1992, pp. 720–733.
19. T.L. Dhami, L.M. Manocha, and O.P. Bahl, *Carbon* **29**(1), 51–60 (1991).
20. I.M.K. Ismail and W.C. Hurley, *Carbon* **30**(3), 419–427 (1992).
21. M. Tagawa, N. Ohmae, M. Umeno, A. Yasukawa, K. Gotoh, and M. Tagawa, *Jpn. J. Appl. Phys.* **30**(9), 2134–2138 (1991).
22. D.H.R. Jenkins and B. McKibbin, *J. Bone Joint Surg.* **62B**(4), 497–499 (1980).
23. A. Cameron and D. Taylor, in *Proc. Institute of Basic Medical Sciences Symp. on Interaction of Cells with Natural and Foreign Surfaces, Royal College of Surgeons of England, 1984*, Plenum Press, New York, 1986, pp. 271–278.
24. T. Khan, M. Dauzvardis, and S. Sayers, *Brain Research* **541**(1), 139–145 (1991).